Stress Intensity Factor calculation from displacement fields

S. Beretta, L. Patriarca, S. Rabbolini
Politecnico di Milano, Department of Mechanical Engineering, via La Masa 1, 20156, Milano, Italy
stefano.beretta@polimi.it, luca.patriarca@polimi.it, silvio.rabbolini@polimi.it

ABSTRACT. In the last two decades, visual image techniques such as Digital Image Correlation (DIC) enabled to experimentally determine the crack tip displacement and strain fields at small scales. The displacements are tracked during loading, and parameters as the Stress Intensity Factor (SIF), opening and closing loads, T-stress can be readily measured. In particular, the SIFs and the T-stress can be obtained by fitting the analytical equation of the Williams-type expansion with the experimentally-determined displacement fields. The results in terms of fracture mechanics parameters strictly depend on the dimension of the area considered around the crack tip in conjunction with the crack length, the maximum SIF (and thus the plastic tip radius), and the number of terms to be considered in the Williams-type expansion. This work focuses in understanding the accuracy of the SIF calculation based on these factors. The study is based on Finite Element Analysis simulations where purely elastic material behavior is considered. The accuracy of the estimation of the SIF is investigated and a guide-line is provided to properly set the DIC measurements. The analysis is then experimentally validated for crack closure measurements adopting the SENT specimen geometry.

KEYWORDS. Stress intensity factor; Digital image correlation; Crack-tip displacement fields.

Citation: Beretta, S.., Patriarca, L., Rabbolini, S., Stress Intensity Factor calculation from displacement fields, Frattura ed Integrità Strutturale, 41 (2017) 269-276.

Received: 28.02.2017
Accepted: 03.05.2017
Published: 01.07.2017

INTRODUCTION

The digital image correlation (DIC) technique is nowadays largely adopted as a reliable, non-destructive, low-cost technique to measure real-time local displacements on a flat surface of the specimens [1, 2]. The full-field displacement and strain measurements found several engineering applications as, for example, in the study of the crack tip fields and in the characterization of the typical fracture mechanics parameters such as the stress intensity factor (SIF). However, the adoption of displacement measurements to calculate the SIFs is critical, and special attention is required to properly select the DIC measurements. For example, the choice of the area of interest in front the crack tip (field-of-view) strictly depends on to the type of the analytical model selected for the fitting of the displacement field. It turns out that the accuracy of the SIFs measurements from full-field DIC displacement fields is a technical issue which still requires attention even though the rich literature growing in the last decades [3-5]. In fact, real crack tip displacement fields are affected by several factors that cannot be easily controlled during DIC displacement measurements. Crack tip plasticity, crack closure, correlation parameters (field of view, subset size) have shown to profoundly influence the SIF calculation. In order to clarify and to provide a guideline on the SIF measurements, in this work we analyze the displacement field calculated according finite element (FE) simulations of two typical cracked body geometries: the center cracked tension (CCT) and single-edge notched tension (SENT) specimens. Starting from the displacement fields obtained from the FE simulations, this work shows the comparison with the SIF predicted by the numerical analyses focusing specifically on the parameters that are required to be properly set to obtain an accurate SIF measurement during DIC measurements. The methodology was successively experimentally implemented for the measurement of the opening stress for a crack propagating in a SENT specimen.

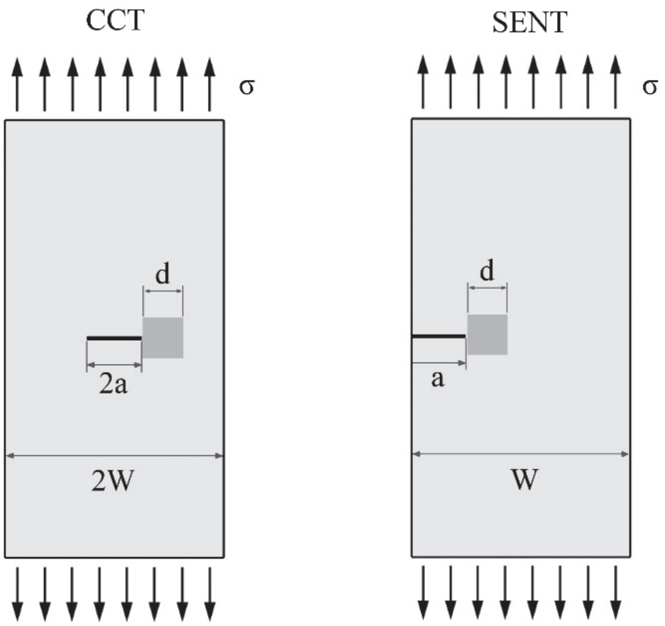

Figure 1: Geometries considered in this study: Center Cracked Tension (CCT) and Single-Edge Notched Tension (SENT) specimens.

The regressions of the displacement fields in front of the crack tip are based on the Williams expansion [6]. The Williams expansion is herein written for the displacements v in the direction perpendicular to the crack surfaces in three different versions based on the number of terms involved:

$$v = \frac{K_I}{2\mu}\sqrt{\frac{r}{2\pi}}\sin\left(\frac{\vartheta}{2}\right)\left[k+1-2\cos^2\left(\frac{\vartheta}{2}\right)\right]+Ar\cos(\vartheta)+B_v \quad (1)$$

$$v = \frac{K_I}{2\mu}\sqrt{\frac{r}{2\pi}}\sin\left(\frac{\vartheta}{2}\right)\left[k+1-2\cos^2\left(\frac{\vartheta}{2}\right)\right]+\frac{T}{8\mu}r\left[k\sin(\vartheta)-3\sin(\vartheta)\right]+Ar\cos(\vartheta)+B_v \quad (2)$$

$$\begin{aligned} v = &\frac{K_I}{2\mu}\sqrt{\frac{r}{2\pi}}\sin\left(\frac{\vartheta}{2}\right)\left[k+1-2\cos^2\left(\frac{\vartheta}{2}\right)\right]+\frac{T}{8\mu}r\left[k\sin(\vartheta)-3\sin(\vartheta)\right]+ \\ &+A_{13}\frac{r^{3/2}}{2\mu}\left[\left(k-\frac{1}{2}\right)\sin\left(\frac{3}{2}\vartheta\right)-\frac{3}{2}\sin\left(\frac{\vartheta}{2}\right)\right]+Ar\cos(\vartheta)+B_v \end{aligned} \quad (3)$$

The terms A and B account the contributions of the specimen rotation and translation on the displacement field.

The CCT and SENT geometries are shown in Fig.. 1. The field-of-view dimension is herein indicated as *d*, while the crack length in indicated as *a* and the specimen width as *W*.

NUMERICAL ANALYSES

Fig. 2 illustrates the preliminary FE analysis performed to set the dimension of the finite element in proximity of the crack tip necessary to model the stress singularity determining the SIF. For a crack length of *a=0.9mm*, and a ratio *a/W=0.3*, the FE simulations show convergence of the stress fields for element sizes in proximity of the crack tip of, respectively, *3.6µm* and *2.5µm*.

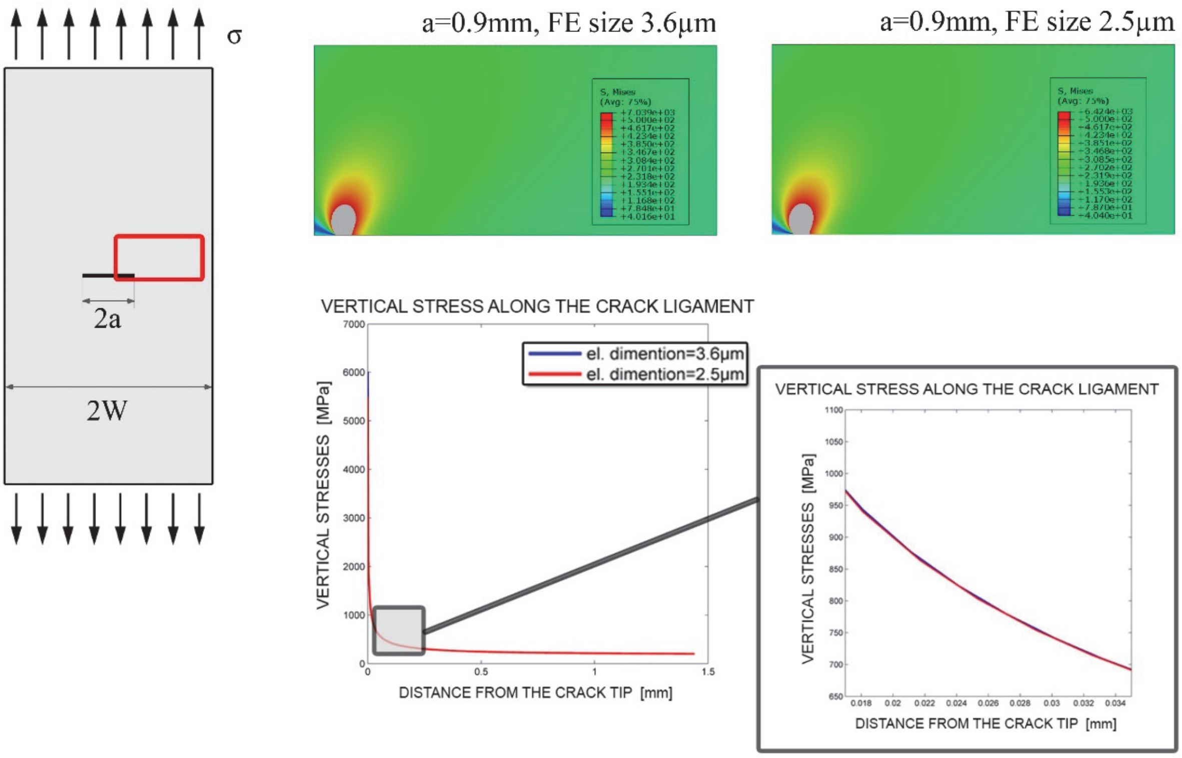

Figure 2: Convergence analysis for finite element model according to finite element sizes of 3.6µm and 2.5µm in proximity of the crack tip. The stress plot indicates that the dimension of the elements chosen provides the same stress distribution.

Following the FE model definition, a set of FE analyses was implemented. The crack lengths analyzed range from *a/W=0.05* to *a/W=0.5*. Fig. 3 shows the results of the regression of the FE displacement fields for different number of terms included in the Williams expansion. The regression adopting only the first term (K) yields to precise SIF estimations only for very restricted field-of-view dimension d (less than *0.01mm*). However, the real material behavior shows local plasticity in front of the crack tip which includes the small area where the K regression provides accurate results. In addition, performing DIC measurements with such small field-of-view is a challenging task and it would involve other problems with out-of-plane displacements that affect the DIC quality. It turns out that the regression based only on the first term of the Williams expansion is not pursued, and the additional terms are required to be fitted. The SIF measurement based on the 2-terms regression is also observed to provide generally inaccurate SIF values. In particular, only for field-of-view dimensions lower than *d<0.2mm* the SIF calculated shows a 10% discrepancy with the FE solution. The 3-terms regression is shown to be the most accurate and stable for field-of-view dimensions raging from *d>0.2mm* to *d=1.4mm* giving an accuracy of less than 5% on the SIF estimation.

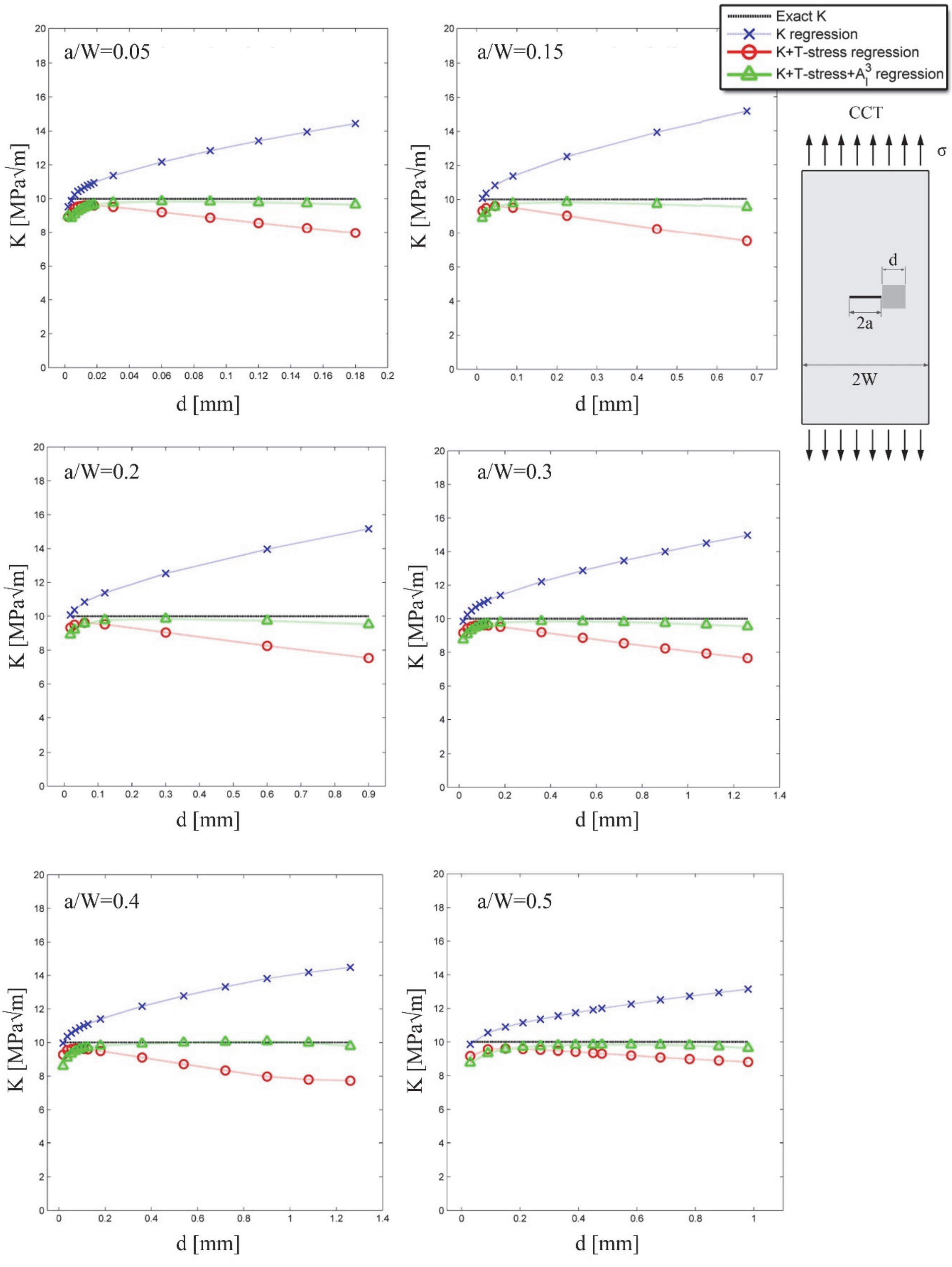

Figure 3: Precision of SIF calculation depending on the crack length and the dimension of the regression region for the CCT specimen. The regression based only on the K term is always overestimating the SIF and only for very small regression regions it gives accurate SIF solutions; the solution including the K term and the T-stress tends to underestimate the SIF, even though the solution is accurate for relative for dimensions of the regression area up to *0.2 mm*. The 3-terms regression results in the most stable and accurate SIF estimations. In particular, it requires regression dimensions higher than *d>0.2mm* which can be adopted in DIC measurements.

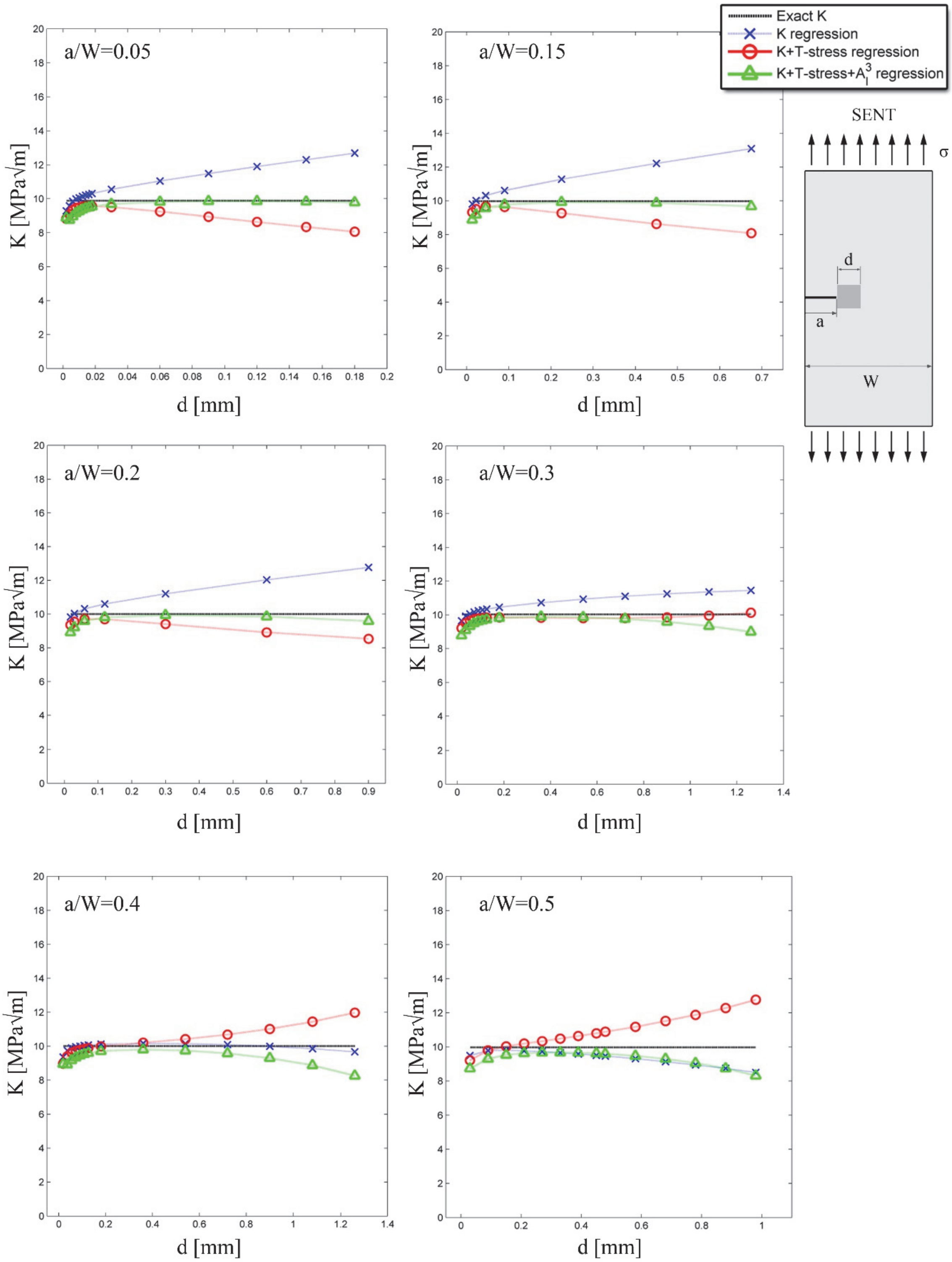

Figure 4: Precision of SIF calculation depending on the crack length and the dimension of the regression region for the SENT specimen. The regression based only on the K term is not accurate for most of the crack lengths investigated, and it gives accurate predictions only for small regression regions *d<0.05mm* which requires high DIC resolutions. The most accurate solutions are given by the 3-terms regression.

Similar trends can be observed for the analyses performed for the SENT geometry, Fig. 4. For field-of-view dimensions lower than *d<0.2mm* the most accurate SIF estimations are given by the single and 2-terms regressions. Again, the regressions presented refer to an idealized linear elastic continuum and do not consider the local plasticity arising from the crack tip. The 3-terms regression is providing also for the SENT geometry the most accurate results for field-of-views larger than *d>0.2mm*. The adoption of larger number of terms to fit the Williams expansion do not improve further the SIF accuracy as already shown by M. Mokhtari and coauthors [1].

EXPERIMENTS

The experimental set-up adopted in the present work is shown in Fig. 5a. A Leica DFC290HD camera was used in conjunction with Optem lens in order to capture real-time in-situ DIC images. The specimens were machined by electrical discharge machining (EDM) to a dog-bone geometry with gauge section of 6mm x 3mm and a lateral notch with 1mm depth. The specimen surfaces in proximity of the notch tip were prepared for DIC measurements. Initially, the target surface was polished with abrasive paper up to a grit of P2500. Successively, a fine speckle pattern was produced using an IWATA airbrush and black paint. A very refined pattern is required for the present analysis, and this was accomplished by using the airbrush with a 0.18mm wide needle. The image resolutions available with this speckle pattern range from 2.13μm/px to 0.53μm/px. The tested alloy is a quenched and tempered high strength 30NiCrMoV12 steel with Young's modulus equal to 207 GPa, yield stress σ_Y=945MPa and ultimate tensile stress σ_u=1023MPa.

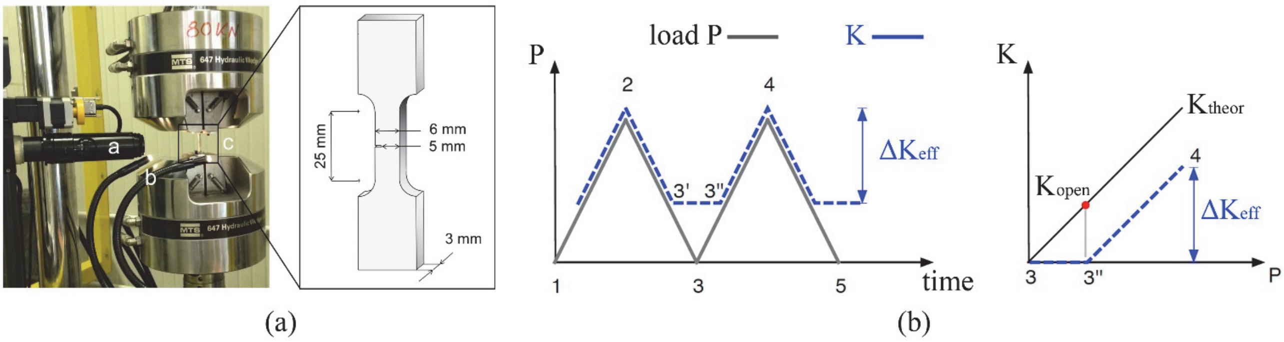

Figure 5: Experimental set-up for DIC measurements: a) The optical microscope, the hydraulic load frame, and the specimen geometry adopted for the present study; b) the crack propagation is affected by the crack closure, the analysis is based on the effective SIF range ΔK_{eff}.

The specimens were cyclically loaded by means of a servo-hydraulic MTS Landmark 810 load frame. The load ratio R was set to 0.05. Initially, the specimens were pre-cracked to a crack length of 1.7mm. Successively, the crack was grown from 1.7mm to a final crack length of 2.58mm and different DIC measurements were performed at different crack advancements (Tab. 1).

a [mm]	K_{theo} [MPa√m]	K_{open} [MPa√m] (2-terms)	K_{open}/K_{theo} (2-terms)	K_{open} [MPa√m] (3-terms)	K_{open}/K_{theo} (3-terms)
1.70	18.65	7.46	0.4	8.01	0.43
1.83	20.25	7.49	0.37	8.50	0.42
1.95	21.83	7.86	0.36	8.30	0.38
2.17	25.09	9.78	0.39	9.53	0.38
2.58	33.77	13.85	0.41	14.18	0.42

Table 1: SIF measurements by DIC displacement field measurements during crack advance.

Fig. 5b depicts the DIC acquisition strategy performed at different crack lengths. The images were acquired during two load cycles. The reference image for correlation is selected as the image captured at minimum load. The images captured successively were correlated using a commercial software (VIC 2D) and the displacement field for each load increment was successively used to calculate the SIF. The SIF evolution with the load P is then plotted and compared with the SIF calculated analytically. It is important to observe that, since the SIF is calculated based on the displacement fields calculated from the reference image captured at the minimum load, the measured SIF is interpreted as a variation ΔK form the reference condition.

Since the crack propagation is also influenced by crack closure, we also provide an analysis of the measured effective ΔK_{eff}. The plot in Fig. 5b shows that the measured SIF remains approximately zero before crack opening which occurs at point 3" where it can be defined the opening SIF as the K_{open}. The ratio between the opening SIF and the maximum SIF calculated analytically K_{open}/K_{theo} is used to quantify the crack closure effect. This approach has been already successfully adopted by Carroll and co-authors [7].

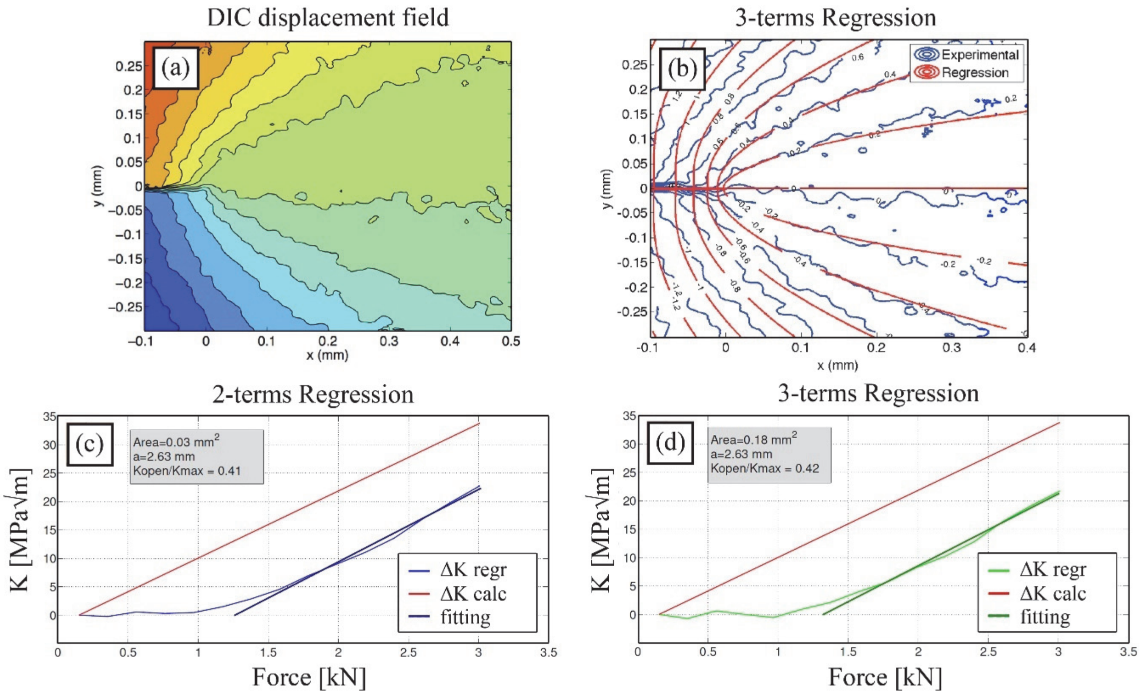

Figure 6: DIC measurements and regression of the displacement field: a) contour plot of the DIC displacement field; b) analysis of the displacement fields by the 3-terms regression; c) ΔK calculation and comparison with the analytical solution for the 2-terms regression and for the d) 3-terms regression. In order to precisely measure the SIFs, the area adopted for the two regressions are different according the analysis performed in the first part of the paper, for more details refer to the text.

Fig. 6 shows the main results of the experiment conducted on the SENT specimen. Contour plot in Fig. 6a shows the vertical displacement field as calculated from the DIC algorithm for a defined load step. Fig. 6b indicates the vertical displacement field (blue lines) and the displacement field calculated from the fitting of the William expansion adopting a correlation basted on the first 3 terms (red lines). Accordingly, Fig. 6c and 6d include the analyses of the variation of the SIF during loading for the same crack length but different number of terms in the regression. In particular, Fig. 6c shows the SIF variation according the 2-terms regression calculated using a DIC regression area of $0.03\ mm^2$ which corresponds to a field-of-view dimension of $d=0.17mm$. The crack length at this test interruption was $a/W=0.4$. According to these parameters, Fig. 4 shows that the SIF calculated should provide accurate results. As a comparison, Fig. 6d shows the 3-terms regression. In this case, the numerical analysis (Fig. 4) suggests that, for a crack length of $a/W=0.4$, the regression performed with 3 terms provides accurate SIF values when the field-of-view dimension is between $d=0.2mm$ and $d=0.6mm$. The DIC regression area was then selected to be $0.18\ mm^2$ which corresponds to a field-of-view dimension $d=0.42mm$. Comparing the results in terms of SIF values it is observed a good agreement between the two types of regressions. This results also in the correct estimation of the closure levels of approx. $K_{open}/K_{theo}=0.4$ for both the types of regressions.

Final remarks

This work focused on the analysis of the field-of-view influence in the SIF calculation from displacement fields measured using the DIC technique. In the first part of the work, numerical analyses on CCT and SENT geometries were designed aiming to reproduce the displacement fields in the crack tip area. The results of the FE simulations enabled to study the influence of the number of terms in the regression of the displacement fields based on the area investigated (field-of-view). This study provides a guideline to properly select the field-of-view dimension and the number of terms in the Williams expansion to obtain accurate SIF evaluation from DIC measurements. Experimentally, a crack was grown in a notched dog-bone specimen (SENT geometry), and the displacement fields were measured with real-time DIC acquisitions for specific crack advancements. The SIFs were determined using 2-terms and 3-terms regressions and compared. Following the first part of the work, two different field-of-views were selected depending on the number of terms selected in the Williams expansion giving a difference in the SIFs estimations within 5%.

References

[1] Mokhtari, M., Lopez-Crespo, P., Moreno, B., Zanganeh, M., Some experimental observations of crack-tip mechanics with displacement data, Frattura ed Integrita Strutturale, (33) (2015) 143.
[2] Hild, F., Roux, S., Measuring stress intensity factors with a camera: Integrated digital image correlation (I-DIC), Comptes Rendus Mécanique 334(1) (2006) 8-12.
[3] Réthoré, J., Gravouil, A., Morestin, F., Combescure, A., Estimation of mixed-mode stress intensity factors using digital image correlation and an interaction integral, International Journal of Fracture, 132(1) (2005) 65-79.
[4] Sutton, M.A., Orteu, J.-J., Schreier, H. W., Image Correlation for Shape, Motion and Deformation Measurements: Basic Concepts, Theory and Applications, (2009).
[5] Pan, B., Qian, K., Xie, H., Asundi, A., Two-dimensional digital image correlation for in-plane displacement and strain measurement: a review, Measurement science and technology, 20(6) (2009) 062001.
[6] Williams, M., On stress distribution at base of stationary crack., Journal of Applied Mechanics 24 (1957) 109.
[7] Carroll, J., Efstathiou, C., Lambros, J., Sehitoglu, H., Hauber, B., Spottswood, S., Chona, R., Investigation of fatigue crack closure using multiscale image correlation experiments, Engineering Fracture Mechanics, 76(15) (2009) 2384-2398.